J Fluoresc (2012) 22:597–608
DOI 10.1007/s10895-011-0995-z

ORIGINAL PAPER

Studies on Curcumin and Curcuminoids. XLVI. Photophysical Properties of Dimethoxycurcumin and Bis-dehydroxycurcumin

L. Nardo · A. Andreoni · M. Bondani · M. Másson · T. Haukvik · H. H. Tønnesen

Received: 10 May 2011 / Accepted: 14 October 2011 / Published online: 27 October 2011

Abstract The steady-state absorption and fluorescence, as well as the time-resolved fluorescence properties of dimethoxycurcumin and bis-dehydroxycurcumin dissolved in several solvents differing in polarity and H-bonding capability are presented. The singlet oxygen generation efficiency of the two compounds relative to curcumin is estimated. The photodegradation quantum yield of the former compound in acetonitrile and methanol is determined. The dimethoxycurcumin and bis-dehydroxycurcumin decay mechanisms from the S_1 state are discussed and compared with those of curcumin, dicinnamoylmethane and bis-demethoxycurcumin.

Keywords Curcuminoid · Fluorescence decay mechanisms · Intramolecular hydrogen bonding · Solute-solvent interactions · Excited state intramolecular proton transfer

Introduction

Curcumin (CURC), the main yellow orange pigment derived from the rhizome of the plant Curcuma longa L., is being extensively studied because of its notable biomedical properties, including anti-inflammatory [1–3], antioxidant [2, 3], chemopreventive [4, 5] and chemotherapeutic [6, 7] potentials. CURC also seems to have a potential in the treatment of Alzheimer disease [8] and cystic fibrosis [9], and is being considered as a model substance for the treatment of HIV-infections [10–12] and as an immune-stimulating agent [10]. Combination with light induces additional biological activities in CURC [13–19]. Upon excitation to the S_1-state CURC becomes phototoxic to bacteria [15–19] and to mammalian cells, both cancerous [14] and healthy [13], via mechanisms that are still to be elucidated [14, 20–23].

As shown in Fig. 1, CURC belongs to the group of β-diketones. Thus, it exhibits tautomerism between enol- and keto- structures, as shown in Fig. 2a and b, respectively. The closed *cis* enol tautomer of *β*-diketones, see Fig. 2a, is characterized by an intramolecular hydrogen bond (H-bond) between the keto and the enol moieties (keto-enol intramolecular H-bond, KEIHB). When the enol group forms the KEIHB, the β-diketone system undergoes

L. Nardo (✉) · A. Andreoni
Department of Physics and Mathematics,
University of Insubria and C.N.I.S.M.-C.N.R.,
Via Valleggio,
11-22100 Como, Italy
e-mail: luca.nardo@uninsubria.it

A. Andreoni
e-mail: andreoni@uninsubria.it

M. Bondani
Institute for Photonics and Nanotechnology,
C.N.R. (Consiglio Nazionale delle Ricerche),
Via Valleggio,
11-22100 Como, Italy
e-mail: maria.bondani@uninsubria.it

M. Másson
Faculty of Pharmaceutical Sciences, School of Health Sciences,
University of Iceland,
Hagi, Hofsvallagata 53,
IS-107 Reykjavik, Iceland
e-mail: mmasson@hi.is

T. Haukvik · H. H. Tønnesen
School of Pharmacy, University of Oslo,
Blindern, P.O.Box 1068, 0316 Oslo, Norway

T. Haukvik
e-mail: Tone.Haukvik@farmasi.uio.no

H. H. Tønnesen
e-mail: h.h.tonnesen@farmasi.uio.no

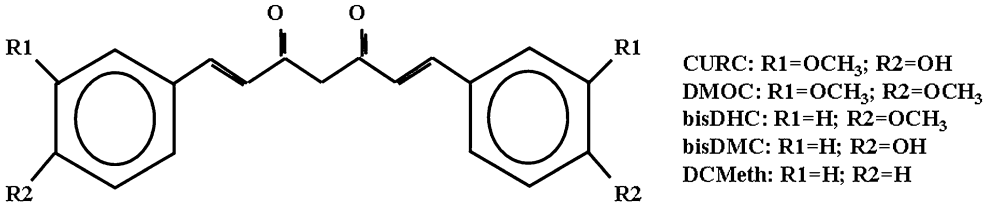

Fig. 1 Chemical structures of the curcuminoids cited in this article

changes towards the total π-system delocalization [24]. There is a strong correlation between the strength of the KEIHB and the π-system delocalization.

Determination of the S_1 dynamics and identification of the deactivation pathways of CURC and other biologically active curcuminoids may be relevant in assessing the molecular mechanisms that lead to the photosensitizing activity. Indeed, assessment of the dependence of the S_1-decay mechanisms on both the molecular substituents and the environmental conditions is a relevant step towards the rational design of synthetic CURC analogues featuring enhanced biological activity, allowing full exploitation of the photosensitizing potential of curcuminoids. Practically, any decay mechanism competing with that triggering the photosensitizing reactions should by inhibited as much as possible. Particularly, any mechanism leading to photo-chemical degradation, which has been reported to be significant for CURC in certain environments [25, 26], would be particularly undesirable.

In a previous work [21], we proposed a model which was capable to explain the data on the decay from the S_1 state of CURC. The following radiationless decay mechanisms were considered to concur with fluorescence emission: (i) direct excited-state intra-molecular proton transfer (ESIPT) from the enol to the keto group of the closed *cis*-enol tautomer [27, 28]; (ii) reketonization [29, 30]; (iii) charge/energy transfer to the solvent molecules [24]; (iv) slow, solvent-rearrangement moderated ESIPT. The latter occurs in case a *trans* enol or open *cis* enol molecule isomerizes to the closed *cis* enol conformer while in the S_1 state, and then decays to S_0 by means of ESIPT [21]. We showed that the fastest non-radiative S_1-decay process for CURC is direct ESIPT. Obviously, the ESIPT rate is the faster the stronger is the KEIHB. The high potential barriers calculated for the exchange of the enol proton in enolized β-diketone systems [27] lead us to postulate that ESIPT can take place only if the KEIHB is formed. Both the polarity of the solvent and its capacity to form intermolecular H-bonds may influence the KEIHB strength: any negative residual charge on the carbonyl oxygen prevents the KEIHB formation and the π-system delocalization whereas intermolecular H-bonding perturbs the KEIHB, [13, 21]. Namely, hydrogen bond donating solvents interact with the keto moiety, while hydrogen bond acceptors interact with the enol proton. Indeed, our conclusion was that the ESIPT process takes place for CURC only in non-polar environment.

Studies on the crystal structure of several symmetric curcuminoids differing as to their phenyl ring substituents indicate that, at least in the solid state, changes in the phenolic moieties influence the electron delocalization and induce differences in the KEIHB strength, as well as in the intermolecular H-bonding capability [31–35]. Similar differences are probably induced in solution as well. As an example, electron-withdrawing groups, such as the methoxy groups in the meta- position of CURC (Hammett constant $\sigma_{OCH_3}^{meta} = 0.12$ [36]), might conjugate with the enol double bond and increase the acidity of the enol proton, thereby strengthening the KEIHB [47]. On the contrary, the phenolic hydroxyl groups in the para- position of CURC (Hammett constant $\sigma_{OH}^{para} = -0.37$ [36]) might exert an overall electron donating effect, induce a decrease in the enol proton acidity and weaken the KEIHB. However, the combined effect of the methoxy and hydroxyl phenolic moieties in CURC might possibly depend on their mutual interactions as well [38], thus the KEIHB strength in CURC is influenced in an unpredictable way.

In order to elucidate the substituents effect on the KEIHB strength, with the aim of gathering preliminary

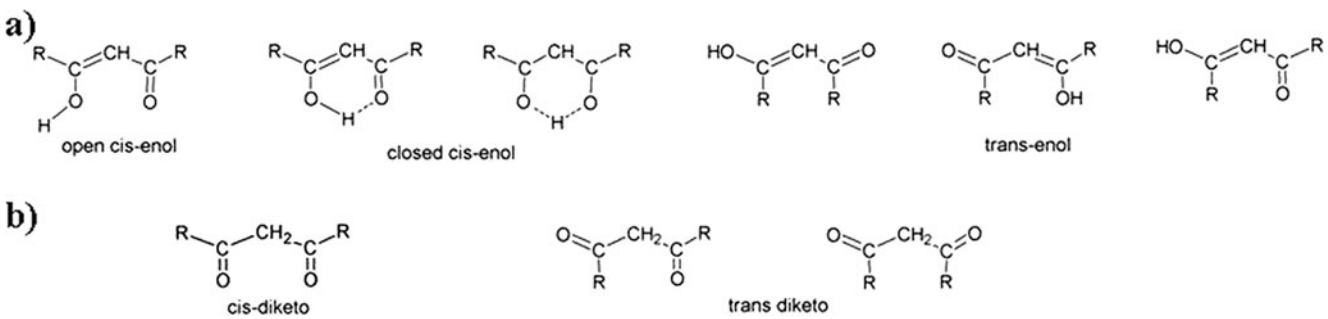

Fig. 2 **a** Enol conformers and **b** diketo conformers of the investigated curcuminoids. For R-structures see Fig. 1

information in view of the design of a photosensitizing drug in which ESIPT will be inhibited, we recently studied the excited-state photophysics of dicinnamoylmethane (DCMeth) [22] and bis-demethoxycurcumin (bisDMC) [23]. It turned out that our model was capable to explain also the very complex phenomenology observed for these two compounds. Moreover, the observed proneness to undergo ESIPT was dramatically enhanced in the case of DCMeth, in which the phenyl rings have a reduced electron donating character with respect to those of CURC and the π-system delocalization of the keto-enol moiety is superior in the solid state [34]. Finally, the ESIPT mechanism was significantly inhibited in the case of bisDMC, whose phenyl rings have a higher tendency to electron donation and whose solid structure suggested the enol proton to be more localized [32, 33].

The present work describes the ground- and excited singlet state characteristics of another two synthetic curcumin analogues, dimethoxycurcumin (DMOC) and bis-dehydroxycurcumin (bisDHC). The structures of DCMeth, bisDMC, DMOC, and bisDHC are sketched in Fig. 1, along with that of the parent compound, CURC. Absorption, steady-state fluorescence and fluorescence decay measurements, performed on HPLC purity degree samples of DMOC and bisDHC dissolved in several solvents differing in polarity and H-bonding capability, are presented. As a preliminary attempt to estimate the relevance of singlet-triplet intersystem crossing as a S_1 deactivation mechanism, the photosensitized singlet oxygen generation efficiency relative to that of CURC is reported in both polar non-protic (acetonitrile) and polar protic (methanol) environment. This data also yield preliminary information on the ability of the two compounds to photosensitize the generation of reactive oxygen species, i.e. of working as conventional photosensitizers for photodynamic therapy. The photodegradation quantum yields of DMOC in acetonitrile and methanol are also reported. The most relevant decay mechanisms of DMOC and bisDHC are identified by taking advantage of our previous studies on CURC [21], DCMeth [22], and bisDMC [23]. The ESIPT rate, and thus the strength of the intramolecular keto-enol H-bond, is shown to decrease at increasing the electron donating character of the phenolic substituents.

Materials and Methods

Chemicals and Sample Preparation

DMOC and bisDHC were synthesized as previously described [39]. All the solvents were ≥99.5% pure and were used as received, except ethyl acetate, which was dried over sodium sulfate. Samples in organic solvents were prepared the same day they were used for measurements.

Absorption and Fluorescence Spectra, Fluorescence Quantum Yield

The UV-VIS absorption spectra were measured by an UV-2401 PC UV-VIS recording spectrophotometer (Shimadzu, Tokyo, Japan).

Steady-state fluorescence measurements were carried out with the PTI modular Fluorescence System (PTI, London, Ontario, Canada) described in [21]. The samples thermostated at 25.0±0.1 °C were excited at 420 nm, which is the wavelength of the laser used as the excitation source in the time-resolved fluorescence measurements. The system was equipped with a software (Felix™ for Windows) performing automatic correction of the acquired spectra with regard to the spectral response of both the excitation lamp and the detector.

Fluorescence quantum yields were determined from the spectrum integrated fluorescence by using, as a reference value, that of quinine sulfate in 0.05 M H_2SO_4 excited at its 344 nm absorption peak: $\Phi_{REF}=0.51$ [40]. The calculated quantum yields were corrected for differences in peak absorbance and in refractive index of the solvents (obtained from the product specification). The reported values are calculated as the average of three parallels, with errors given by the maximum spread between the experimental data.

Fluorescence-Decay Measurements

The fluorescence decays were detected by Time-Correlated Single-Photon Counting (TCSPC). The used TCSPC setup has ~30 ps time resolution (full width at half maximum of the detected excitation pulse) and is fully described elsewhere [21–23, 41]. The fluorescence of the solutions, which were contained in a 1×1 cm^2 fluorimeter quartz cuvette, was excited at 420 nm by the second harmonic (SH) output of a mode locked Ti:sapphire laser (Tiger-ps SHG, Time Bandwidth Products, Zurich, CH). The fluorescence at λ>500 nm was collected at 90° to the excitation beam through a cut-off filter (LL-500, Corion, Holliston, MA) by a 20X microscope objective and focused onto the sensitive area of a PDM50 single-photon avalanche diode (Micro-photon-devices, Bolzano, IT). All fluorescence decays were collected up to 10,000 peak counts in strict single photon regime by suitably attenuating the excitation beam with neutral-density filters. The maximum absorbance of the solutions at the excitation wavelength was 0.05.

Six decay curves were acquired for each sample. The fluorescence decay data were fitted, without deconvolving the system pulse response, to either single or triple

exponentials above a constant background, by minimizing the chi-square value through a Levenberg-Marquardt algorithm. The number of exponential components was established by adding, one by one, exponential components to the fitting function until the fitting routine converged to yield two components of equal time constant. The means of the values obtained from the fits of the six parallels, with errors given by the standard deviations, were assumed as the time constant, τ_i, and initial amplitude, A_i, of the i-th decay component, being the A_i values calculated at the peak channel of the experimental data.

Luminescence Detection of Singlet Oxygen

The generation of singlet oxygen ($^1O_2$) was measured by steady-state detection of luminescence at 1270 nm. A PTI modular Fluorescence System (PTI, London, Ontario, Canada) equipped with an EQ-817 Germanium Detection system operated under liquid nitrogen conditions was used [21].

Photodegradation Quantum Yields

The photodegradation quantum yield of DMOC in selected solvents was measured using the potassium ferrioxalate chemical actinometer [42]. The samples were irradiated by using a monochromator (Applied Photophysics Ltd., f 3.4, 900 W xenon arc lamp) operated with a bandwidth of 20 nm at the selected wavelength. The number of sample molecules reacted per unit time and per unit volume as a function of exposure time was quantified by means of reversed phase HPLC. The separation was performed on a 150×3.9 mm Nova Pak® C_{18} column (Waters, Milford, USA). The mobile phase was a mixture of acetonitrile and 0.5% citric acid buffer, adjusted to pH 3 with KOH. The samples were detected at 350 nm. This detection wavelength was selected in order to reveal tentative degradation products. The chromatic system consisted of a LC-9A pump, a SP D-10A UV-VIS detector, a SIL-10 DV auto sampler and a C-R3A integrator (Shimadzu, Japan). Similar measurements were not undergone for bisDHC due to poor solubility of the compound in the above solvents.

Results

The solvents used in the present study were divided into the following categories: non-polar (cyclohexane), polar weakly H-bonding (chloroform, ethyl acetate, acetone, acetonitrile), strong H-bond acceptors (dimethylformamide, DMFA, and dimethylsulfoxide, DMSO), and alcohols (isopropanol, ethanol, methanol, and ethylene glycol). The dielectric constant ε was adopted as the indicator of the solvent polarity. The Kamlet acidity parameter α and basicity parameter β, were used as the indicators of the solvent H-bond donating and accepting properties, respectively [43]. The above-mentioned solvent properties are summarized in Table 1.

Steady-State Absorption and Emission

The absorption maxima, λ_{Abs}, of DMOC and bisDHC in the different solvents are listed in Table 2a and b, respectively. Some representative spectra are displayed in Fig. 3a and b, respectively. In all solvents except cyclohexane the absorption spectra were broad and essentially structureless. In the case of DMOC, the absorption maximum was significantly blue-shifted with respect to that of CURC [21] in all the strongly H-bonding solvents (minimum blue shift 5 nm in DMSO and ethylene glycol, maximum blue shift 10 nm in isopropanol), while in polar weakly H-bonding solvents we observed values equal within 1–2 nm. In the case of bisDHC a systematic blue shift with respect to CURC was observed in all the solvents (in analogy with bisDMC). In cyclohexane the main absorption band displays two peaks. This is consistent with observations made for CURC [21], DCMeth [22] and bisDMC [23]. In the case of DMOC each of the peaks are slightly red shifted compared to the corresponding CURC peak, while for bisDHC they are both blue shifted. For both compounds a systematic red shift was observed when changing from cyclohexane to solvents with higher dielectric constants. However, unlike CURC [21] and bisDMC [23], a further red shift from weaker to stronger H-bonding solvents of comparable polarity was not observed. From a quantitative standpoint, there was no linear correlation between either ε, α or β and λ_{Abs}.

Table 1 Solvent properties: hydrogen bonding donor parameter, α; hydrogen bonding acceptor parameter, β; dielectric constant measured at 20 °C, ε

Solvent		ε	α	β
Non polar	Cyclohexane	2.02	0	0
Polar weakly H-bonding	Chloroform	4.81	0.44	0
	Ethyl acetate	6.02	0	0.45
	Acetone	20.60	0.08	0.48
	Acetonitrile	38.8	0.19	0.31
Strong H-bond acceptors	DMFA	37.6	0	0.69
	DMSO	48.9	0	0.76
Alcohols	Isopropanol	19.92	0.78	0.95
	Ethanol	25.07	0.83	0.77
	Methanol	33.62	0.93	0.62
	Ethylene glycol	37.70	0.90	0.52

Table 2 Absorption and fluorescence emission maxima, λ_{Abs} and λ_{Fl} (excitation wavelength: 420 nm), and Stokes shifts, $\Delta\tilde{\nu}$, of dimethoxycurcumin (DMOC) in a) and of bis-dehydroxy-curcumin, bisDHC in b)

Solvent		λ_{Abs} (nm)	λ_{Fl} (nm)	$\Delta\tilde{\nu}(10^3\ cm^{-1})$
a				
Non polar	Cyclohexane	410, 432	505, 473, 445	–
Polar weakly H-bonding	Chloroform	421	492	3.5
	Ethyl acetate	418	492	3.6
	Acetone	419	510	4.3
	Acetonitrile	419	521	4.7
Strong H-bond acceptors	DMFA	423	522	4.4
	DMSO	429	530	4.4
Alcohols	Isopropanol	421	534	5.1
	Ethanol	421	542	5.3
	Methanol	417	554	5.9
	Ethylene glycol	428	562	5.6
b				
Non polar	Cyclohexane	404, 425	492, 466, 438	–
Polar weakly H-bonding	Chloroform	414	473	3.1
	Ethyl acetate	409	478	3.5
	Acetone	411	486	3.7
	Acetonitrile	410	486	3.8
Strong H-bond acceptors	DMFA	417	494	3.8
	DMSO	420	503	3.9
Alcohols	Isopropanol	412	502	4.4
	Ethanol	412	507	4.6
	Methanol	412	513	4.8
	Ethylene glycol	421	525	4.8

The fluorescence spectra of both DMOC and bisDHC are broad and essentially structureless in all solvents except cyclohexane, in which three emission maxima were identified. This is consistent with observations made for CURC and bisDMC. Some representative spectra are displayed in Fig. 4a and b for DMOC and bisDHC, respectively. The emission maxima, λ_{Fl}, are listed in Table 2a and b, respectively. In cyclohexane, the two compounds display Stokes shifts of each of the three fluorescence peaks almost identical to those measured for CURC. In the other solvents, the Stokes shifts measured for DMOC (see Table 2a are roughly similar to those measured for CURC [21] (maximum difference 5000 cm^{-1} in chloroform). On the other hand, the bisDHC fluorescence spectra are notably blue-shifted compared to the CURC spectra [21], so that the Stokes shifts are smaller for bisDHC than for CURC (and DMOC) in all solvents (the minimum differential Stokes shift between bisDHC and CURC is 4000 cm^{-1} in ethyl acetate, the maximum difference is 11000 cm^{-1} in methanol).

The fluorescence quantum yield, Φ_{Fl}, of DMOC (Table 3a) is generally higher than that of bisDHC (Table 3b), with only two exceptions: methanol and ethylene glycol. For both compounds, the lowest Φ_{Fl} value was obtained in cyclohexane. A similar result was obtained for CURC [21]. However, CURC had higher Φ_{Fl} values in the polar, weakly H-bonding solvents (ranging from Φ_{Fl}= 0.094 in chloroform to Φ_{Fl}=0.174 in acetone) than in the strongly H-bonding solvents (from Φ_{Fl}=0.022 in ethylene glycol to Φ_{Fl}=0.041 in DMFA), with the only exception of isopropanol (Φ_{Fl}=0.114) [21]. In contrast, the quantum yields of DMOC are not significantly dependent from the H-bonding properties of the solvent. Moreover, DMOC exhibits the maximum Φ_{Fl} in the strong H-bond acceptor DMSO (Φ_{Fl}=0.218, see Table 3a). On the other hand, bisDHC exhibits the maximum Φ_{Fl} in ethylene glycol, which is a strongly H-bonding solvent (Φ_{Fl}=0.182, see Table 3b), and the Φ_{Fl} values seem to be generally somewhat higher in strongly than in weakly H-bonding solvents.

Excited-State Dynamics

The decay times, τ_i, together with the relative initial amplitudes, A_i, as determined by the multi-exponential fits of the fluorescence decays of DMOC and bisDHC are reported in Table 4a and b, respectively. Average fluorescence lifetimes τ_{av} were calculated for each solvent as $\tau_{av} = \sum_i \tau_i A_i / \sum_i A_i$ and are reported in Table 3a and b for the sake of comparison to the Φ_{Fl} data. The radiative (k_{Fl}) and

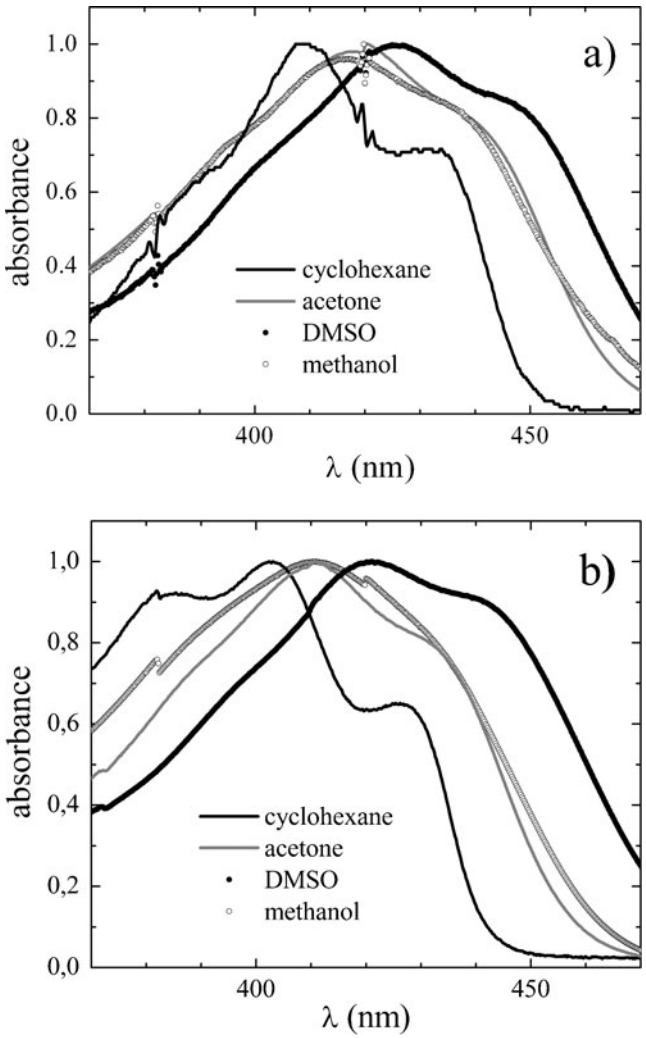

Fig. 3 **a** Absorption spectra of **a** dimethoxycurcumin (DMOC) and **b** bisdehydroxycurcumin (bisDHC) in cyclohexane (*solid black line*), acetone (*solid grey line*), DMSO (*full dots*) and methanol (*empty circles*)

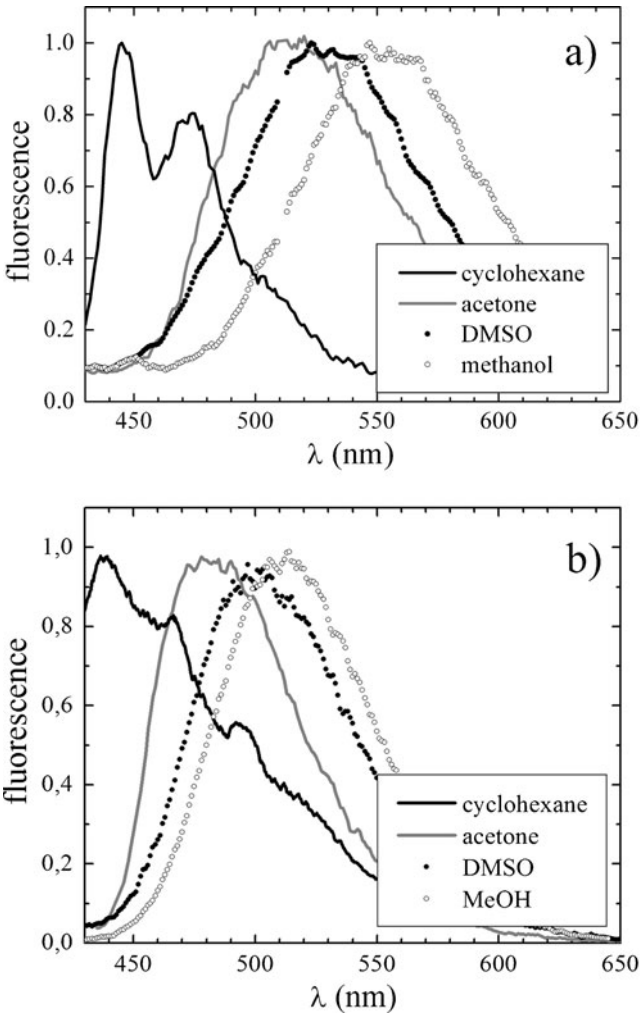

Fig. 4 **a** Fluorescence emission spectra of **a** dimethoxycurcumin (DMOC) and **b** bisdehydroxycurcumin (bisDHC) in cyclohexane (*solid black line*), acetone (*solid grey line*), DMSO (*full dots*) and methanol (*empty circles*)

non-radiative (k_{NR}) rate constants were calculated from the Φ_{Fl} and τ_{av} values listed in Table 3a and b according to the following equations:

$$k_{Fl} = \frac{\Phi_{Fl}}{\tau_{av}} \tag{1}$$

$$k_{NR} = \frac{1}{\tau_{av}} - k_{Fl} \tag{2}$$

The obtained values are reported in the same Tables. The values of k_{NR} are substantially higher than the corresponding k_{Fl} values in all solvents for both compounds. Thus, it can be concluded that the deactivation of S_1 occurs predominately via non-radiative pathways. This is consistent with previous observations on CURC [21], DCMeth [22], and bisDMC [23]. Three exponential components were resolved in the fluorescence decay of both DMOC and bisDHC in cyclohexane, like for CURC and bisDMC. Both DMOC and bisDHC display single-exponential decays in all the other solvents. This behavior is similar to that observed for bisDMC, and very different from that of CURC, for which two decay components were identified in all the strongly H-bonding solvents except isopropanol (in which a single exponential decay was observed).

The k_{Fl} values for DMOC and bisDHC are very similar for the two compounds and from a solvent to the other. They are also comparable to those calculated in the case of CURC [21]. The only exception to this rule is observed in cyclohexane, where the k_{Fl} value calculated for DMOC is similar to that of bisDMC [23], i.e., more than twice the value calculated for bisDHC, which in turn is very similar to that calculated for CURC.

Table 3 Photophysical properties of a) DMOC and b) bisDHC in the different solvents. Fluorescence quantum yield, Φ_{Fl}; average fluorescence decay time (see text for details), τ_{av}; radiative and non-radiative decay rates, k_{Fl} and k_{NR}, as calculated from Eq. 1 and Eq. 2, respectively. Quantum yield of photodegradation, Φ_{Degr} (only for DMOC in acetonitrile and methanol)

Solvent		Φ_{Fl}	τ_{av} (ps)	k_{Fl} (10^9 s^{-1})	k_{NR} (10^9 s^{-1})	Φ_{Degr}
a						
Non polar	Cyclohexane	0.012±0.001	66	0.18	14.97	
Polar weakly H-bonding	Chloroform	0.141±0.004	566	0.25	1.52	
	Ethyl acetate	0.116±0.004	489	0.24	1.80	
	Acetone	0.189±0.001	757	0.25	1.07	
	Acetonitrile	0.202±0.004	862	0.23	0.93	0.101±0.005
Strong H-bond acceptors	DMFA	0.127±0.007	893	0.14	0.98	
	DMSO	0.218±0.007	888	0.25	0.88	
Alcohols	Isopropanol	0.186±0.004	936	0.20	0.87	
	Ethanol	0.155±0.010	689	0.22	1.23	
	Methanol	0.049±0.014	418	0.12	2.27	0.059±0.008
	Ethylene glycol	0.079±0.012	410	0.19	2.25	
Solvent		Φ_{Fl}	τ_{av} (ps)	k_{Fl} (10^9 s^{-1})	k_{NR} (10^9 s^{-1})	
b						
Non polar	Cyclohexane	0.0060±0.0003	97	0.063	10.25	
Polar weakly H-bonding	Chloroform	0.067±0.002	292	0.22	3.20	
	Ethyl acetate	0.033±0.002	196	0.17	4.93	
	Acetone	0.067±0.003	276	0.24	3.38	
	Acetonitrile	0.077±0.004	317	0.24	2.91	
Strong H-bond acceptors	DMFA	0.064±0.006	392	0.16	2.39	
	DMSO	0.132±0.001	478	0.28	1.81	
Alcohols	Isopropanol	0.102±0.003	466	0.22	1.92	
	Ethanol	0.134±0.001	549	0.24	1.58	
	Methanol	0.088±0.008	580	0.15	1.57	
	Ethylene glycol	0.182±0.008	818	0.22	1.00	

This similarity in the k_{Fl} values displayed by different curcuminoids even in very different environments suggests that the decay photophysics, as well as the Φ_{Fl} and τ_{av} values, are mainly dictated by the rates of the non-radiative decay processes.

The k_{NR} values measured for DMOC spanned from $k_{NR}=0.87\times10^9$ s^{-1} in isopropanol to $k_{NR}=14.97\times10^9$ s^{-1} in cyclohexane. The values were very similar in weakly and strongly H-bonding solvents. The k_{NR} values measured for bisDHC spanned from $k_{NR}=1.00\times10^9$ s^{-1} in ethylene glycol to $k_{NR}=10.48\times10^9$ s^{-1} in cyclohexane. They were generally higher in weakly H-bonding solvents than in strongly H-bonding solvents (similarly to what observed for bisDMC [23] and opposite to that observed for CURC [21]). Moreover, in the polar weakly H-bonding solvents the k_{NR} values calculated for bisDHC (and bisDMC) were more than twice as high as the corresponding values calculated for CURC [21] and DMOC, while in strongly H-bonding solvents the k_{NR} values were comparable for DMOC, bisDHC, and bisDMC [23] and much higher for CURC [21].

Singlet Oxygen Generation

As for CURC [21], also for DMOC and bisDHC we observed barely detectable singlet oxygen luminescence signals in both acetonitrile and methanol. Besides indicating that the three compounds are very modest $^1O_2$ generators, the above results also suggest that at least in these solvents S_1 deactivation through intersystem crossing dynamics is negligible. Singlet oxygen is most efficiently produced by DMOC dissolved in acetonitrile. The relative amounts of $^1O_2$ produced with respect to DMOC in acetonitrile (1) are: 0.44 for DMOC in methanol; 0.73 and 0.19 for CURC; 0.08 and 0.14 for bisDHC, in acetonitrile and methanol, respectively.

Photodegradation Quantum Yields

The quantum yield of photodegradation, Φ_{Degr}, of DMOC was measured in acetonitrile and methanol (Table 3a). It is significantly higher than that measured for CURC [21] in the same solvents (acetonitrile: $\Phi_{Degr}=0.061$ ±0.011;

Table 4 Decay times, τ_i±standard deviation (ps), and relative initial amplitudes, A_i, that fit the experimental fluorescence decays of a) CURC and b) bisDMC in the different solvents (i=1 to 3)

Solvent		$\tau_1(A_1)$	$\tau_2(A_2)$	$\tau_3(A_3)$
a				
Non polar	Cyclohexane	49±3 (.89)	208±2 (.11)	864±27 (<.01)
Polar weakly H-bonding	Chloroform	566±4 (1)		
	Ethyl acetate	489±7 (1)		
	Acetone	757±3 (1)		
	Acetonitrile	862±6 (1)		
Strong H-bond acceptors	DMFA	893±3 (1)		
	DMSO	888±1 (1)		
Alcohols	Isopropanol	936±1 (1)		
	Ethanol	689±3 (1)		
	Methanol	418±2 (1)		
	Ethylene glycol	410±2 (1)		
b				
Non polnar	Cyclohexane	59±3 (.80)	250±10 (.20)	1334±100 (<.01)
Polar weakly H-bonding	Chloroform	292±3 (1)		
	Ethyl acetate	196±1 (1)		
	Acetone	276±3 (1)		
	Acetonitrile	317±2 (1)		
Strong H-bond acceptors	DMFA	392±2 (1)		
	DMSO	478±2 (1)		
Alcohols	Isopropanol	466±3 (1)		
	Ethanol	549±3 (1)		
	Methanol	580±5 (1)		
	Ethylene glycol	818±6 (1)		

methanol: 0.021±0.010). However, in acetonitrile $\Phi_{Degr} \cong 1/2\Phi_{Fl}$ and in methanol it is only slightly higher than Φ_{Fl}. Thus, in neither of these solvents photochemical decomposition is the most relevant deactivation mechanism of S_1 for DMOC.

Discussion

In references [21–23] we proposed a model which was capable to explain the data on the decay from the S_1 state of CURC and its analogues DCMeth and bisDMC. It was postulated that the curcuminoids in solution at room temperature are essentially present in their enol conformers only (see Fig. 2a, in agreement with previous studies [20, 37, 44–46]. For both CURC and bisDMC, the H-bonded closed *cis* enol structure is dominant in non-polar environments, while either the open *cis* enol or the *trans* enol conformers, which cannot form the KEIHB, are dominant in polar weakly H-bonding and polar strongly H-bonding solvents, respectively [21, 23, 37]. Tiny amounts of the minimally polar *trans (anti)* diketo conformer (see Fig. 2b) can be found in non-polar environments [44]. Conversely, DCMeth, which is endowed with a much stronger KEIHB and undergoes almost complete π-system delocalization, is mostly present in the closed *cis* enol conformer in all of the solvents, as evidenced by the substantial inertness of its spectroscopic parameters with respect to the solvent properties and by the very fast non-radiative decay rate, which was interpreted as the capacity of transferring the enol proton by direct ESIPT regardless to the environment.

The results of the above-mentioned works can be used as a guideline in ascribing a decay mechanism to each of the exponential components of the DMOC and bisDHC fluorescence decays detected in the various solvents. The quantum yield and decay data suggest that all the tested curcuminoids decay through the same deactivation pathways in cyclohexane. Moreover, alike the curcuminoids that we previously studied [21–23], also DMOC and bisDHC display minimum Stokes shifts in cyclohexane, which is a symptom of KEIHB formation and consequent prevention of out-of-plane vibrations. Hence, the three decay components observed for both DMOC and bisDHC in cyclohexane are ascribed to: (i) decay through direct ESIPT (τ_1 in Table 4a and b); (ii) de-excitation by reketonization (τ_2); (iii) radiative decay of the *trans (anti)* diketo conformer (τ_3). Interestingly, a comparison of the decay data concerning the five analyzed curcuminoids in cyclohexane, which is the most inert solvent

among those used in the present studies, yields valuable information about the relative efficiency of the ESIPT mechanism, and consequently on the strength of the unperturbed KEIHB. Such a comparison should take into account that ESIPT occurs only through the low-activation-potential reaction coordinate pathway for the four substituted curcuminoids: CURC, bisDMC, DMOC, and bisDHC. Conversely, in the case of the non-substituted CURC analogue DCMeth the high-activation-potential direct transfer pathway is also followed, due to the superior symmetry of its semiaromatic ring. For a full discussion on these two ESIPT mechanisms we refer to [22] and references therein. Obviously, the latter decay mechanism is slower, and this reduces the overall k_{NR} of DCMeth. However, the superior strength of the KEIHB in this compound, whose phenyl rings are the least electron donating, is testified by the presence of major components of the fluorescence decay ascribed to direct ESIPT in all the solvents. For the other compounds, the calculated k_{NR} values can be considered to be good approximations of the ESIPT rate through the reaction coordinate pathway, which is the main decay mechanism. Notably, there is a good linear correlation (R^2= 0.9869, see Fig. 5a) between the k_{NR} values and the electron donating character of the phenyl rings, quantified by means of the sum of the Hammett parameters of the phenolic substituents. Moreover, including also DCMeth, both the decay times of the components associated to ESIPT through the reaction coordinate pathway (Fig. 5b) and the fraction of molecules decaying through ESIPT (in the case of DCMeth expressed by the sum of the relative amplitudes of the decay components associated to both ESIPT mechanisms, see Fig. 5c) roughly correlate with the electron donating character of the phenyl rings (R^2=0.87 and R^2=0.93, respectively). These results seem to suggest that the strength of the KEIHB is primarily dictated by the electron donating character of the phenyl rings.

The lack of a decay component with lifetime as fast as the τ_1 measured in cyclohexane in both weakly- and strongly H-bonding polar solvents suggests that KEIHB is perturbed and direct ESIPT does not occur in these solvents in the cases of DMOC and bisDHC. This is consistent with observations made on CURC and bisDMC [21, 23]. The KEIHB seems to be so strong as to survive in any environment only in the case of DCMeth, which may be ascribed to the superior delocalization of its π-system and with the relatively weakly electron donating phenyl rings. The single exponential decays obtained for both DMOC and bisDHC in the polar, weakly H-bonding solvents indicate that, similarly to what was observed for CURC and bisDMC, the only relevant non-radiative decay mechanism in such solvents is solvent-rearrangement moderated ESIPT. DMOC decay times and quantum yields in these solvents are similar to those measured for CURC. Conversely, bisDHC shows shorter decay times and lower quantum yields, which are very similar to those measured in the case of bisDMC. Thus, solvent rearrangement seems to be faster for the latter curcuminoids, indicating an overall S_1 excited state molecular dipole moment lower than that of

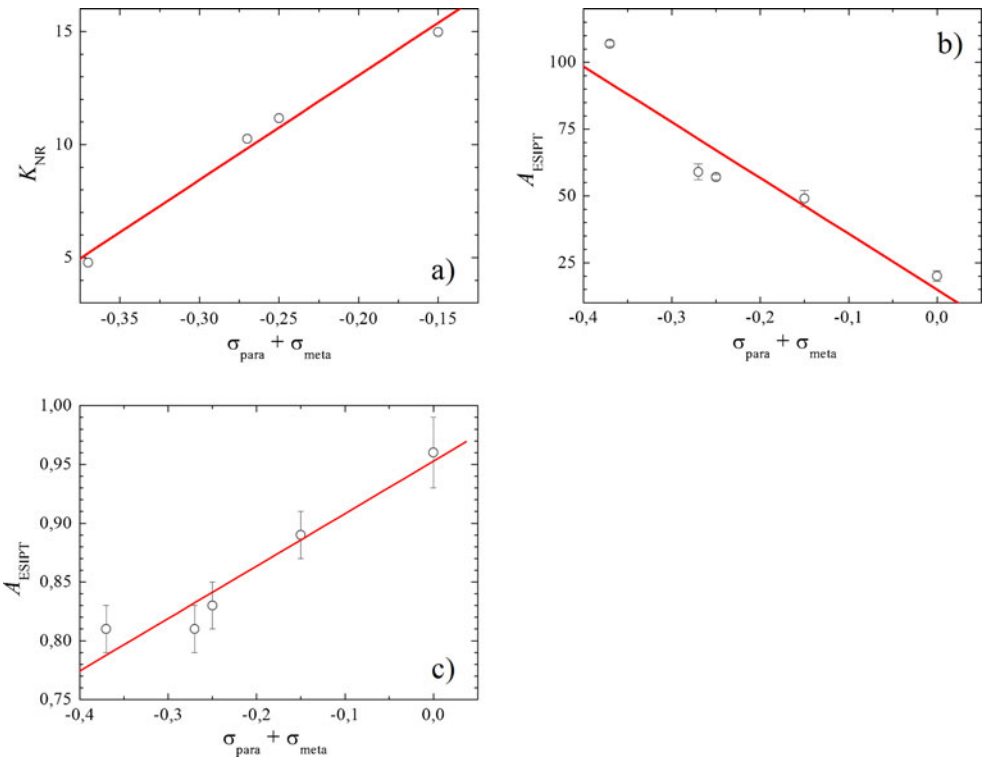

Fig. 5 Plots of **a** the non-radiative decay rate, k_{NR}, (DCMeth excluded); **b** the time constant of the decay component ascribed to ESIPT through the reaction coordinate path; **c** the fraction of molecules decaying by ESIPT; measured for the curcuminoids of Fig. 1 dissolved in cyclohexane, versus the electron donating character of their phenyl rings (expressed in terms of Hammett constants of the phenyl substituents)

CURC and DMOC. Indeed, the S_1 dipole moment of CURC has been reported to be exceptionally high, and, in particular much higher that that of other curcuminoids, including, e.g., DCMeth [47]. Interestingly, in none of the three compounds the time needed for solvent-rearrangement moderated ESIPT to take place does not monotonically increase at increasing the solvent dielectric constant. It should be noted, however, that also the solvent viscosity, η, has a relevant role in establishing both the desolvation and the proton transfer kinetics. This might explain, e.g., why in chloroform (η=0.58 cP) we observed slower decay dynamics than in ethyl acetate (η=0.45 cP) for both DMOC and bisDHC. The situation is further complicated by the non-completely negligible and solvent-dependent tendency of all the considered weakly-H-bonding solvents to form H-bonds (see α and β values in Table 1).

In the strongly H-bonding solvents, both DMOC and bisDHC have slower decay and higher fluorescence quantum yield than CURC. The lack of a decay component with time constant of the same order of magnitude as that of the shortest CURC decay component suggests that, as observed for bisDMC, inter-molecular H-bond formation does not induce alternative mechanisms of deactivation of the excited state. Indeed, the τ_1-values measured for DMOC and bisDHC in strongly H-bonding solvents are in the range of those ascribed to decay by means of solvent rearrangement moderated ESIPT for either CURC, bisDMC, or DCMeth [21–23]. In the case of DMOC the value was typically longer than that measured for CURC and similar to those measured for bisDMC and DCMeth, indicating tighter inter-molecular H-bonding in H-bonding solvents for DMOC compared to CURC keto-enol moiety. However, while for bisDMC the interaction with H-bond donors and acceptors was similarly strong [23], DMOC, like DCMeth [22], seems to interact preferentially with H-bond acceptors. Conversely, with the exception of the very long decay time measured for bisDHC in ethylene glycol, the decay data suggest that solvent rearrangement moderated ESIPT occurs for bisDHC and CURC in strongly H-bonding solvents, on the same, faster time scale.

Even though H-bonding solvents seem to interact only weakly with the CURC keto-enol moiety, intermolecular H-bond mediated decay by charge/energy transfer is observed exclusively for this compound. This observation suggests that this decay mechanism should involve the phenolic hydroxyl moieties of CURC rather than its keto or enol groups. Indeed, it has been shown [47, 48] that both deprotonation and electron transfer occur at the phenyl rings. Obviously, as both DMOC and bisDHC lack hydroxyphenyl groups, they cannot undergo similar excited-state reactions. The detection, in H-bonding solvents, of small amounts of DCMeth decaying with a time constant similar to that of the component ascribed to decay by intermolecular charge/energy transfer in CURC [21, 22] might indicate that in DCMeth the enolic proton is more acidic than in CURC, and has a pKa similar to that of the CURC phenolic hydroxyl protons.

Conclusion

The excited-state dynamics of the curcuminoids DMOC and bisDHC were investigated by means of steady-state absorption and fluorescence and fluorescence decay measurements performed on the compounds dissolved in several solvents of different polarity and H-bonding capability. The decay mechanisms of both compounds from the S_1 state were elucidated and compared with those of CURC, DCMeth and bisDMC. Information about the relative strength of the KEIHB in the unperturbed molecular structures of the five curcuminoids has been derived from the measured rates of decay by means of direct ESIPT in inert solvent. The KEIHB strength has been shown to decrease as the electron donating character of the phenolic substituents increases.

In polar solvents the KEIHB is disrupted in the case of both DMOC and bisDHC. The same holds true for CURC and bisDMC, but not for DCMeth. Neither DMOC nor bisDHC excited states seem to decay through mechanisms mediated by intermolecular-H-bond formation which were demonstrated for CURC in strongly H-bonding solvents.

The photodecomposition of DMOC seems to be faster than that of CURC under similar conditions. Consequently, modification of the CURC molecule by substitution of the hydroxyl with methoxy groups, while increasing the S_1-state lifetime, thus improving the photosensitizing potential, reduces the photostability of the sensitizer. On the other hand, removal of the hydroxyl substituents (such as in bisDHC) results in a significant increase of the S_1-state lifetime only in strongly H-bonding solvents. The consequences for photostability were not investigated due to limited solubility of bisDHC in the actual solvents.

References

1. Mukhopadhyay A, Basu N, Ghatak N, Gujzal PK (1982) Anti-inflammatory and irritant activities of curcumin analogs in rats. Agents Actions 12:508–515
2. Srimal RC, Dhawan BN (1973) Pharmacology of di-ferulyl methane (curcumin), a non-steroidal anti-inflammatory agent. J Pharm Pharmacol 25:447–452
3. Rao T, Basu N, Ghatak N, Gujral PK (1982) Anti-inflammatory activity of curcumin analogs. Indian J Med Res 75:574–578
4. Khafif A, Schantz SP, Chou TC, Edelstein D, Sacks PG (1998) Quantification of chemopreventive synergism between epigallocatechin-3-gallate and curcumin in normal, premalignant

and malignant human oral epithelial cells. Carcinogenesis 19:419–424
5. Leu TH, Maa MC (2002) The molecular mechanisms for the antitumorigenic effect of curcumin. Curr Med Chem 2:357–370
6. Woo J, Kim Y, Choi Y, Kim D, Lee K, Bae JH, Chang DS, Jeong YJ, Lee YH, Park J, Kwon TK (2003) Molecular mechanisms of curcumin-induced cyclotoxicity: induction of apoptosis through generation of reactive oxygen species, down-regulation of Bcl-XL and IAP, the release of cytochrome c and inhibition of Akt. Carcinogenesis 24:1199–1208
7. Moos PJ, Edes K, Mullally J, Fitzpatrick J (2004) Curcumin impairs tumor suppressor p53 function in colon cancer cells. Carcinogenesis 9:1611–1617
8. Yang F, Lim GP, Begum AN, Ubeda OJ, Simmons MR, Ambegaokar SS, Chen P, Kayed R, Glabe CG, Frautschy SA, Cole GM (2004) Curcumin inhibits formation of amyloid β oligomers and fibrils, binds plaques, and reduces amyloid in vivo. J Biol Chem 280:5892–5901
9. Egan ME, Pearson M, Weiner SA, Rajendarn V, Rubin D, Glochner-Pagel J, Canney S, Du K, Lukacs GL, Caplan MF (2004) Curcumin, a major constituent of turmeric, corrects cystic fibrosis defects. Science 304:600–602
10. Aggrawal BB, Sundaram C, Malani N, Ichikawa H (2007) Curcumin: the Indian solid gold. Adv Exp Med Biol 595:1–75
11. Mazumder A, Neamati N, Sunder S, Schulz J, Perez H, Aich E, Pommier Y (1997) Curcumin analogs with altered potencies against HIV-1 integrase as probes for biochemical mechanisms of drug action. J Med Chem 40:3057–3063
12. Sui Z, Salto R, Li J, Craik C, Ortiz de Montellano PR (1993) Inhibition of the HIV-2 proteases by curcumin and curcumin boron complexes. Bioorg Med Chem 1:415–422
13. Bruzell E, Morisbak E, Tønnesen HH (2005) Studies on curcumin and curcuminoids. XXIX. Photoinduced cytotoxicity of curcumin in selected aqueous preparations. Photochem Photobiol Sci 4:523–530
14. Dahl TA, Bilski P, Reszka KJ, Chignell CF (1994) Photocytotoxicity of curcumin. Photochem Photobiol 59:290–294
15. Dahl TA, Mcgowan WM, Shand MA, Srinivasan VS (1989) Photokilling of bacteria by the natural dye curcumin. Arch Microbiol 151:183–185
16. Tonnesen HH, de Vries H, Karlsen J, van Henegouwen GB (1987) Studies on curcumin and curcuminoids IX: investigation of the photobiological activity of curcumin using bacterial indicator systems. J Pharm Sci 76:371–373
17. Haukvik T, Bruzell E, Kristensen S, Tønnesen HH (2009) Photokilling of bacteria by curcumin in different aqueous preparations. Studies on curcumin and curcuminoids. XXXVII. Pharmazie 64:666–673
18. Haukvik T, Bruzell E, Kristensen S, Tønnesen HH (2010) Photokilling of bacteria by curcumin in selected polyethylene glycol 400 (PEG 400) preparations. Studies on curcumin and curcuminoids XLI. Pharmazie 65:600–606
19. Haukvik T, Bruzell E, Kristensen S, Tønnesen HH (2011) A screening for antibacterial phototoxic effects of curcumin derivatives. Studies on curcumin and curcuminoids. XLIII. Pharmazie 66:69–74
20. Chignell CF, Bilski P, Reszka KJ, Motton AG, Sik RH, Dahl TA (1994) Spectral and photochemical properties of curcumin. Photochem Photobiol 59:295–302
21. Nardo L, Paderno R, Andreoni A, Haukvik T, Màsson M, Tønnesen HH (2008) Studies on curcumin and curcuminoids XXXII. Role of H-bond formation in the photoreactivity of curcumin. Spectroscopy 22:187–198
22. Nardo L, Andreoni A, Bondani M, Màsson M, Tønnesen HH (2009) Studies on curcumin and curcuminoids XXXIV. Photophysical properties of a symmetrical, non-substituted curcumin analogue. J Photochem Photobiol B: Biol 97:77–86
23. Nardo L, Andreoni A, Haukvik T, Màsson M, Tønnesen HH (2011) Studies on curcumin and curcuminoids XXXIX. Photophysical properties of bisdemethoxycurcumin. J Fluorescence 21:627–635
24. Gilli G, Bertolasi V (1990) In: Rappoport Z (ed) The chemistry of enols. Wiley, New York, pp 713–764
25. Tønnesen HH, Karlsen J, van Henegouwen GB (1986) Studies on curcumin and curcuminoids. VIII. Photochemical stability of curcumin. Z Lebensm Unters Forsch 183:116–122
26. Sundaryono A, Nourmamode A, Gardrat C, Grelier S, Bravic G, Chasseau D, Castellan A (2003) Studies on the photochemistry of 1,7-dipehnyl-1,6-heptadiene-3,5-dione, a non-phenolic curcuminoid model. Photochem Photobiol Sci 2:914–920
27. Emsley J (1984) In: Clarke MJ, Goodenough JB, Ibers JA, Jørgensen CK, Mingos DMP, Neilands JB, Reinen D, Sadler PJ, Weiss R, Williams RJP (eds) Structure and bonding. Springer Verlag, Berlin, pp 148–191
28. Strandjord AJG, Courtney SH, Friedrich DM, Barbara PF (1983) Excited-state dynamics of 3-hydroxyflavone. J Phys Chem 87:1125–1133
29. Weedon AC (1990) In: Rappoport Z (ed) The chemistry of enols. Wiley, New York, pp 591–638
30. Nikolov P, Fratev F, Petkov I, Markov P (1981) Dimer fluorescence of some β-dicarbonyl compounds. Chem Phys Lett 83:170–173
31. Tønnesen HH, Karlsen J, Mostad A (1982) Structural studies of curcuminoids. I. The crystal structure of curcumin. Acta Chem Scand B 36:475–479
32. Tonnesen HH, Karlsen J, Mostad A, Pedersen U, Rasmussen PB, Lawesson SO (1983) Structural studies of curcuminoids. II. Crystal structure of 1,7-Bis(4-hydroxyphenyl)-1,6-heptadiene-3,5-dione – Methanol complex. Acta Chem Scand B 37:179–185
33. Tonnesen HH, Karlsen J, Mostad A, Pedersen U, Rasmussen PB, Lawesson SO (1988) Structural studies of curcuminoids. IV. Crystal structure of 1,7-Bis(4-hydroxyphenyl)-1,6-heptadiene-3,5-dione Hydrate. Acta Chem Scand B 42:23–27
34. Mostad A, Pedersen U, Rasmussen PB, Lawesson SO (1983) Structural studies on curcuminoids. III. Crystal structure of 1,7-diphenyl-1,5-heptadiene-3,5-dione. Acta Chem Scand B 37:901–905
35. Gorbitz CH, Mostad A, Pedersen U, Rasmussen PB, Lawesson SO (1986) Structural studies on curcuminoids. V. Crystal structures of 1,7-bis(3,4-dimethoxyphenyl)-4-benzyl-1,6-heptadiene-3,5-dione (DDBHDD) and 1,7-bis(4-hydroxy-3-methoxyphenyl)-4-(2-oxo-2-ethoxyethyl)-1,6-heptadiene-3,5-dione (DHMEDD). Acta Chem Scand B 40:420–429
36. Hansch C, Leo A, Taft RW (1991) A survey of Hammett substituent constants and resonance and field parameters. Chem Rev 91:165–195
37. Toullec J (1990) In: Rappoport Z (ed) The chemistry of enols. Wiley, New York, pp 324–398
38. Semenov SG, Khodyreva NV (1994) Theoretical study of electron-donor and spectroscopic properties pf substituted phenols in various solvents. J Mol Struct 337:89–97
39. Tomren MA, Màsson M, Loftsson T, Tønnesen HH (2007) Studies on curcumin and curcuminoids. XXXI. Symmetric and asymmetric curcuminoids: stability, activity and complexation with cyclodextrin. Int J Pharm 338:27–34
40. Velapoldi R, Tønnesen HH (2004) Corrected fluorescence spectra and quantum yields for a series of compounds in the visible spectral region. J Fluorescence 14:465–472
41. Nardo L, Bondani M, Andreoni A (2008) DNA-ligand binding mode discrimination by characterizing fluorescence resonance

energy transfer through lifetime measurements with picosecond resolution. Photochem Photobiol 84:101–110
42. Moore DE (2004) In: Tønnesen HH (ed) Photostability of drugs and drug formulations. CRC, Boca Raton, pp 49–53
43. Kamlet MJ, Abboud JLM, Abraham MH, Taft RW (1983) Linear solvation energy relationships. 23. A comprehensive collection of the solvatochromic parameters, π^*, α, and β, and some methods for simplifying the generalized solvatochromic equation. J Org Chem 48:2877–2887
44. Balasubramanian K (2006) Molecular orbital basis for yellow curry spice curcumin's prevention of Alzheimer's disease. J Agric Food Chem 54:3512–3520
45. Pedersen U, Rasmussen PB, Lawesson SO (1985) Synthesis of naturally occurring curcuminoids and related compounds. Liebigs Ann Chem 8:1557–1569
46. Ortica F, Rodgers MAJ (2001) A laser flash photolysis study of curcumin in dioxane-water mixtures. Photochem Photobiol 74:745–751
47. Galasso V, Kovac B, Modelli A, Ottaviani MF, Pichierri F (2008) Spectroscopic and theoretical study of the electronic structure of curcumin and related fragment molecules. J Phys Chem A 112:2331–2338
48. Wright JS (2002) Predicting the antioxidant activity of curcumin and curcuminoids. J Mol Struct (THEOCHEM) 591:207–217